

Use of HPHT Autoclave to Determine Corrosion Inhibition by Berberine extract on Carbon Steels in 3.5% NaCl Solution Saturated with CO₂

Yuanhua Lin¹, Ambrish Singh^{1,2,*}, Eno E. Ebenso³, M. A. Quraishi⁴, Ying Zhou¹, Yun Huang¹

¹ State Key Laboratory of Oil and Gas Reservoir Geology and Exploitation, Southwest Petroleum University, Chengdu- 610500, Sichuan, China.

² Department of Chemistry, School of Civil Engineering, LFTS, Lovely Professional University, Phagwara-144402, Punjab, India.

³ Department of Chemistry, School of Mathematical & Physical Sciences, North-West University(Mafikeng Campus), Private Bag X2046, Mmabatho 2735, South Africa.

⁴ Department of Applied Chemistry, Indian Institute of Technology, Banaras Hindu University, Varanasi -221 005 India.

*E-mail: vishisingh4uall@gmail.com

Received: 27 May 2014 / Accepted: 1 October 2014 / Published: 17 November 2014

Roots extract of *Coptis chinensis* (Berberine extract) was characterized using gas chromatography (GC) and Fourier transform infrared spectroscopy (FTIR) methods. The influence of berberine extract on corrosion of carbon steels (J55, N80, P110SS and C110 steels) in 3.5 wt.% NaCl solution saturated with CO₂ was evaluated using static high pressure and high temperature (HPHT) autoclave. The surface was further evaluated by X-ray diffraction (XRD), scanning electron microscopy (SEM), and contact angle measurements. Quantum chemical calculations have been used to evaluate the structural, electronic, and reactivity parameters of the inhibitor on the steels surface. SEM, XRD, and contact angle measurement studies reveal that the surface of metals are quite unaffected after use of inhibitor in 3.5% NaCl solution saturated with CO₂.

Keywords: *Coptis chinensis*; Quantum calculations; Contact Angle Measurement; SEM; XRD

1. INTRODUCTION

Carbon steels are the most commonly used material of construction for petroleum production assets. Carbon steels are susceptible to severe corrosion in process environments containing carbon dioxide [1]. Natural gas is most likely contains carbon dioxide as part from reservoir fluid composition while in other hand CO₂ can be injected for enhanced oil recovery purposes. As such, corrosion control

in carbon dioxide containing media is area of concern for oil field industries. Extensive investigation studies had been carried out to understand and control CO₂ corrosion [2]. CO₂ dissolves in oil wells produced water forming carbonic acid that in turn dissociates and decrease the solution pH:



CO₂ and H₂S gases in combination with water are the main cause of corrosion in oil and gas production. In addition, it is normal practice to re-inject production water downhole to maintain the reservoir pressure and stability as well as perform water flooding (using seawater or fresh water sources) to drive oil out of the formation. As field ages, the ratio of watery oil in the produced fluids increases and can reach levels of 95% or higher [3]. This rise in water content implies an increase of the corrosion problems. Internal corrosion caused by the produced fluids is the most costly of the corrosion problems in the oil and gas industry since internal mitigation methods cannot be easily maintained and inspected. Therefore, as a field ages, corrosion control becomes more expensive. Approximately 60% of oilfield failures are related to CO₂ corrosion mainly due to inadequate predictive capability and the poor resistance of carbon and low alloy steels to this type of corrosive attack [4]. CO₂ can produce not only general corrosion but also localized corrosion, which is a much more serious problem.

In China, oil and gas field with CO₂ content is mainly distributed in Songliao basin, Bohai gulf basin, Subei-Nanhuanghai basin, Sichuan basin, and Jilin basin. In Songliao region, the CO₂ content of some gas field is as high as 99.02%. Gas fields in Bohai gulf basin and Jilin basin also contains high CO₂. Puguang gas field is the highest CO₂ content gas field in Sichuan area, with proportion of 7.94-9.07%. In order to enhance oil recovery in Jilin oil field, liquid CO₂ is injected into the formation followed by the hot water. Hence the liquid CO₂ and hot water will be miscible to drive the oil out of the formation, which is called miscible displacement to improve oil recovery. However, the CO₂ dissolved in water will lead to severe carbon dioxide corrosion.

Several chemical compounds have been tested for corrosion inhibition of metals and alloys; however, the compounds having N, S, and O heteroatoms, incorporated in an aromatic system, have been found to possess excellent anticorrosion potential. Because of increasing ecological awareness and strict environmental regulations, as well as the inevitable drive toward sustainable and environmentally benign processes, attention now has been focused on the development of nontoxic alternatives to inorganic and organic inhibitors applied so far [5-9]. In present study we have used root extract of *Coptis chinensis*, which is a native plant of China to extract an isoquinoline alkaloid dye named berberine as shown in Figure 1. We extracted berberine a yellow dye from the root, which is rich in heteroatoms and has also been commonly used as a non-toxic antibiotic for years in China. It is the only cationic dye among the natural plant dyes that is part of the chemical group of isoquinoline alkaloids [10]. The molecules are rich in heteroatoms (O, N, S) which are present in an effective corrosion inhibitor. Inhibition effect of berberine extract on the corrosion of carbon steels in 3.5% NaCl solution saturated with CO₂ was studied using high pressure and high temperature autoclave. Meanwhile, the steel surface was examined by contact angle, XRD, and SEM techniques.

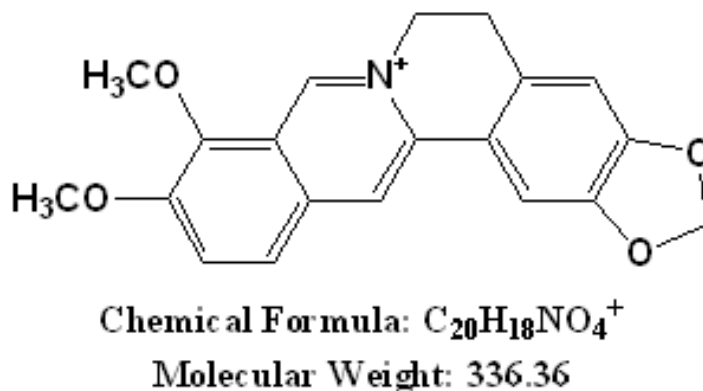


Figure 1. Structure of berberine.

2. EXPERIMENTAL

2.1. Preparation of berberine extract

The roots of the *Coptis chinensis* plant were collected from the field, and the roots were dried and powdered for extraction. Fifty grams of the powder was soaked in 900 ml of reagent grade ethanol for 24 h and refluxed for 5 h. The ethanolic solution was filtered and concentrated to 500 ml. Berberine the yellow colored powder was obtained after vacuum drying the solution. The powder was then refluxed in 3.5% NaCl to prepare the stock solution. This solution was used to study the corrosion inhibition properties.

2.2. HPHT Autoclave weight loss method

A static high pressure and high temperature (HPHT) autoclave was used for the weight loss experiments. The HPHT tests uses a metal cage spindle tightly packed with the cover containing flat specimens and the 3.5% NaCl solution. 3 liters of 3.5% NaCl solution was saturated with CO_2 at a pressure of 6 MPa, temperature of $120^\circ C$ and kept for 7 days (168 hours) to observe the corrosion rate. All the carbon steel coupons were metallographically abraded according to ASTM A262, with fine grade emery papers from 600 to 1200 grade to get a to mirror finish and weighed before inserting them into the HPHT autoclave. At completion of the test, the apparatus are allowed to cool. After 7 days the specimens were washed with double distilled water, followed by acetone, and dried thoroughly. Specimens were then inspected, and re-weighed. A corrosion rate in calculated for a specific test time and weight loss. The 3.5% NaCl solution was prepared by dilution of analytical grade NaCl with double distilled water. This test has been extensively used in developing corrosion inhibitors for applications where ultra-high shear conditions caused severe corrosion in oil and gas pipelines.

Corrosion tests were performed on a J55 steel of the following percentage composition (wt.%): C 0.24; Si 0.22; Mn 1.1; P 0.103; S 0.004; Cr 0.5; Ni 0.28; Mo 0.021; Cu 0.019; Fe balance. P110SS steel having the following chemical composition (wt %): C 0.27; Si 0.26; Mn 0.6; P 0.009; S 0.003; Cr 0.5; Ni 0.25; Mo 0.6; Nb 0.05; V 0.005; Ti 0.02; Fe balance were used for all studies. N80 steel having

the following chemical composition (wt %): C 0.31; Si 0.19; Mn 0.92; P 0.010; S 0.008; Cr 0.2; Fe balance were used for all studies. C110 steel having the following chemical composition (wt %): C 0.35; Mo 0.25; Mn 1.2; Ni 0.99; P 0.02; S 0.005; Cr 1.5; Fe balance were used for all studies.

2.3. Characterization of Berberine

2.3.1. Fourier Transform Infrared Spectroscopy (FTIR)

FTIR was carried out by using Fourier Transform Infrared Spectrometer model NICOLET 6700 connected with OMNIC software. The dried and powdered berberine was mixed with KBr, and grinded in agar-mortar, and then mounted onto a metal case that was used for the study.

2.3.2. Gas Chromatography (GC) Analysis

GC analyses were carried out using a GC-2010 Plus, (Shimadzu Japan) GC apparatus equipped with a single injector and two flame ionization detectors (FID). The apparatus was used for simultaneous sampling to two fused-silica capillary columns (60 m × 0.22 mm, film thickness 0.25 µm) with different stationary phases: (polydimethylsiloxane) and (polyethylene glycol). Temperature program: the oven temperature was programmed from 60°C to 200°C and then held isothermally at 200 °C (20 min).

2.4. Surface Analyses

2.4.1. UV-Visible spectroscopy

The 3.5% NaCl solution saturated with CO₂ containing 1000 ppm of berberine extract before and after immersion of carbon steel strips for 168 hours was subjected to UV-Visible absorption detection using UV-5100 double beam spectrophotometer. The solution containing carbon steel strips incubated in the berberine extract (1000 ppm) was taken out followed by thorough dip washing in water. The berberine extract without carbon steels and the washing solution obtained through dip washing of carbon steels were subjected to UV-Visible absorption detection.

2.4.2. X-Ray Diffraction (XRD)

The carbon steel specimens were immersed in 3.5% NaCl solution saturated with CO₂ in absence and presence of inhibitor for a period of 7 days. After then, the specimens were taken out and dried. The film formed on the surface of the steel specimens was analyzed by using X-ray diffractometer, X Pert PRO incorporated with Higscore software.

2.4.3. Contact Angle Measurement

Contact angle measurements were performed using sessile drop technique using DSA100 Kruss optical contact angle measurement instrument made in Germany. Carbon steel samples were carefully cleaned to avoid the surface contaminations, which influence the contact angle measurements through contamination of the liquid when the latter is put in to contact with the sample surface.

2.4.4. Scanning Electron Microscopy (SEM)

The electrodes were immersed in 3.5% NaCl solution saturated with CO₂ in the absence and presence of corrosion inhibitor to observe the effect of corrosion and inhibition. The carbon steel electrodes were then dried at ambient temperature. Micrographs of abraded and corroded carbon steel surfaces and those after inhibitor addition were taken using a SEM model TESCAN VEGA II XMH instrument.

2.5. Quantum chemical calculations

Quantum chemical calculations were performed using density function theory (DFT) method, B3LYP with electron basis set 6-31G* (d, p) for all atoms. All the calculations were executed with Gaussian 03, E .01. The following quantum chemical indices namely energy of HOMO, LUMO, and dipole moment (μ) was determined [11].

3. RESULTS AND DISCUSSION

3.1 Characterization of Berberine extract

3.1.1. Fourier Transform Infrared Spectroscopy (FTIR)

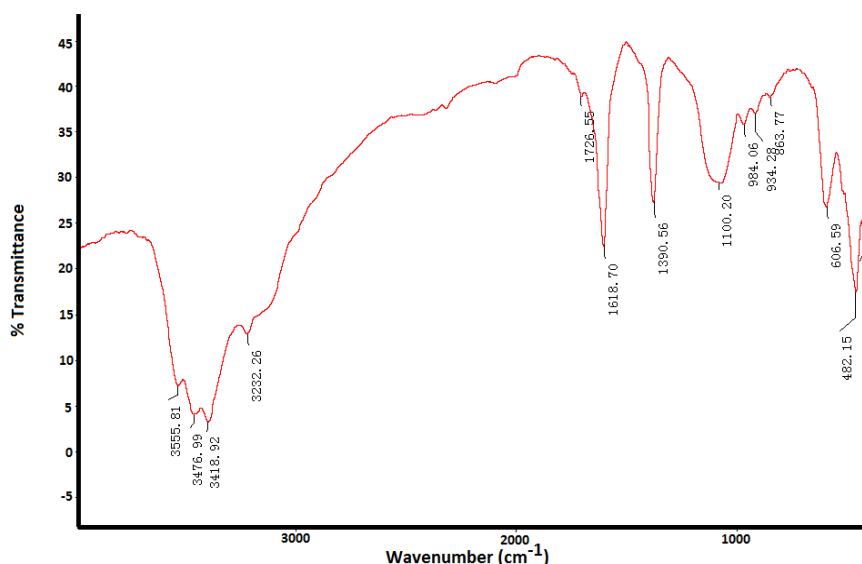


Figure 2. FTIR analysis of Berberine extract

The peaks obtained as in Figure 2 are 482.15 -Br group; 606.59 C-H bending; 863.77 C-N stretching; 934.28 -OH group; 984.06 C-O bending; 1100.20 C-O stretching; 1390.56 C=C (Aromatic); 1618.70 C=C (Aromatic); 1726.55 C=O stretching; 3232.26 N-H stretching; 3418.92 -OH groups; 3476.99 OH-NH stretching vibration; 3555.81 -OH groups.

3.1.2. Gas Chromatography (GC) Analysis

Carrier gas used in the process was He (1 mL/min). Injector and detector temperatures were held at 200 °C. Split injection was conducted with a ratio split of 1:50. Relative component concentrations were calculated based on GC peak areas without using correction factors. A number of prominent peaks were identified in the repeated GC analyses of the berberine extract and the result is shown in Figure 3. Among the peaks identified, they are very similar to alkaloids and close to GC of berberine.

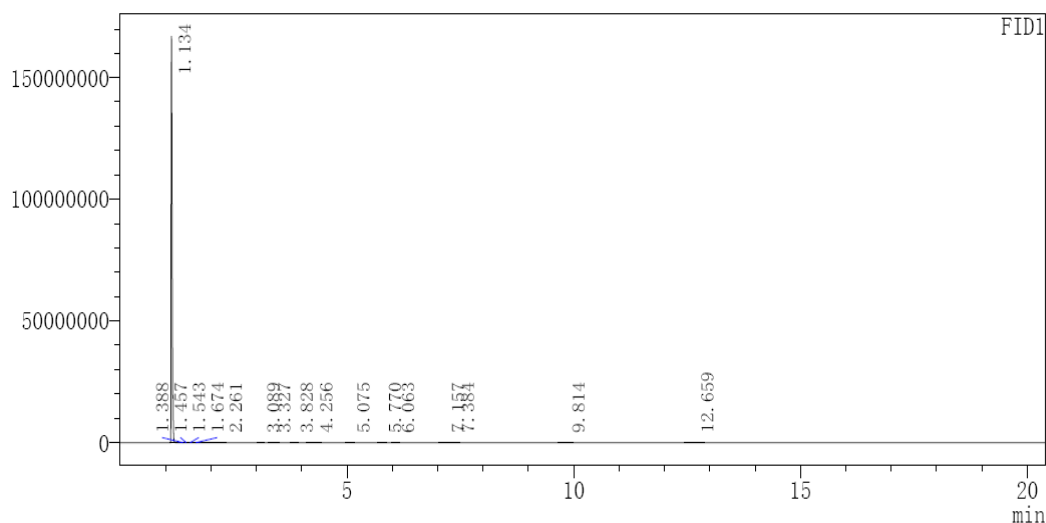


Figure 3. GC analysis of Berberine extract.

3.2. HPHT Autoclave weight loss test

Table 1. Corrosion parameters for different steels in 3.5% NaCl in presence and absence of berberine extract from weight loss measurements at 120°C after 7 days

Steels	Weight loss (mg cm ⁻²)	C _R (mm y ⁻¹)	η (%)
C110 with 3.5% NaCl	64	0.341126	-
C110 with inhibitor	25	0.076372	60
P11OSS with 3.5% NaCl	50	0.287932	-
P11OSS with inhibitor	11	0.051828	78
N80 with 3.5% NaCl	49	0.282173	-
N80 with inhibitor	04	0.023035	92
J55 with 3.5% NaCl	51	0.293691	-
J55 with inhibitor	02	0.017276	96

To study the effect of inhibitor concentration (5 mL/L) on the inhibition efficiency, weight loss experiments were carried out in 3.5% NaCl solution saturated with CO₂ at 120°C for 7 days (168 hours) immersion period. The berberine extract showed inhibition efficiency of 60% for C110 steel, 78% for P110SS steel, 92% for N80 steel and maximum inhibition efficiency of 96% for J55 steel. Triplicate samples of carbon steel were used to get the accurate values of corrosion rate and inhibition efficiency. The values of percentage inhibition efficiency ($\eta\%$) and corrosion rate (C_R) obtained from weight loss method of berberine extract at 120°C are summarized in Table 1.

3.3. Surface Analyses

3.3.1. UV-Visible Spectroscopy Analysis

UV-Visible spectroscopy provides strong evidence for the formation of a metal complex [12]. We obtained UV-Visible absorption spectra for optimum concentration of berberine extract before and after 168 hours immersion of steel specimens. The electronic absorption spectrum of berberine extract before the steels immersion shows two bands in UV-region as depicted in Figure 4. These bands may arise due to π - π^* and n - π^* transitions with a considerable charge transfer character. After 168 hours immersion of steel samples change in the position of absorption maximum or change in the values of absorbance indicate the formation of a complex between two species in solution. However, there was no significant change in the shape of the spectra. These observations provide a strong evidence of complex formation between inhibitor molecules and steel surface and formation of a protective film of inhibitor on the steel surface.

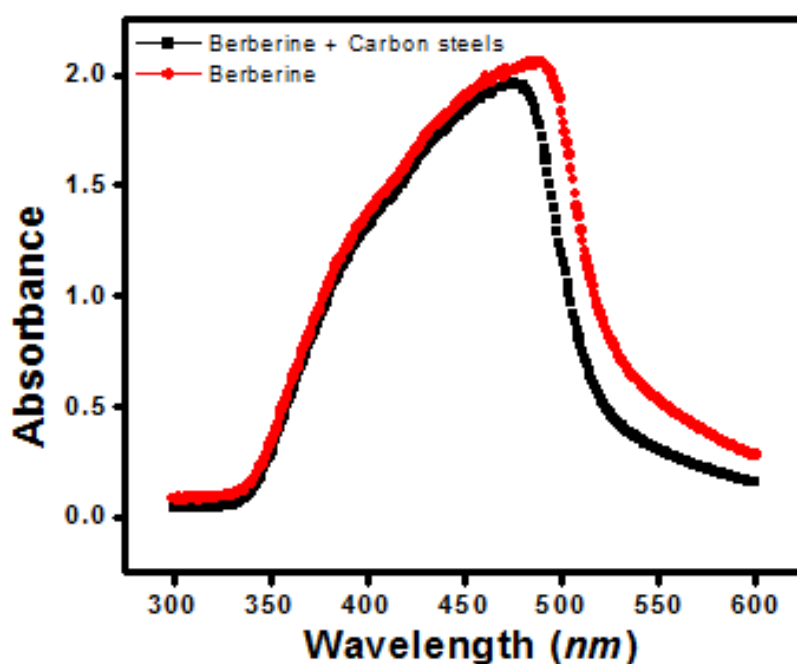


Figure 4. UV-Visible analysis of Berberine extract on J55 steel.

3.3.2. X-Ray Diffraction (XRD)

X-ray diffraction was used to determine the corrosion product and film formation on the carbon steel samples in 3.5% NaCl solution saturated with CO₂. The corrosion product over the surface of the carbon steel samples is shown in Figure 5a. Peaks at $2\theta = 26^\circ, 30^\circ, 38^\circ, 42^\circ, 45^\circ, 50^\circ, 52^\circ, 63^\circ,$ and 69° can be assigned to the oxides of iron. Thus, it is observed that in absence of inhibitor, the surface of the metal contains iron oxides of iron. The XRD patterns of inhibited surface (Figure 5b) showed the presence of iron peaks only, the peaks due to oxides of iron are found to be absent [13, 14]. The formation of adsorbed protective film on the surface of metal in the presence of berberine extract is clearly reflected from these observations.

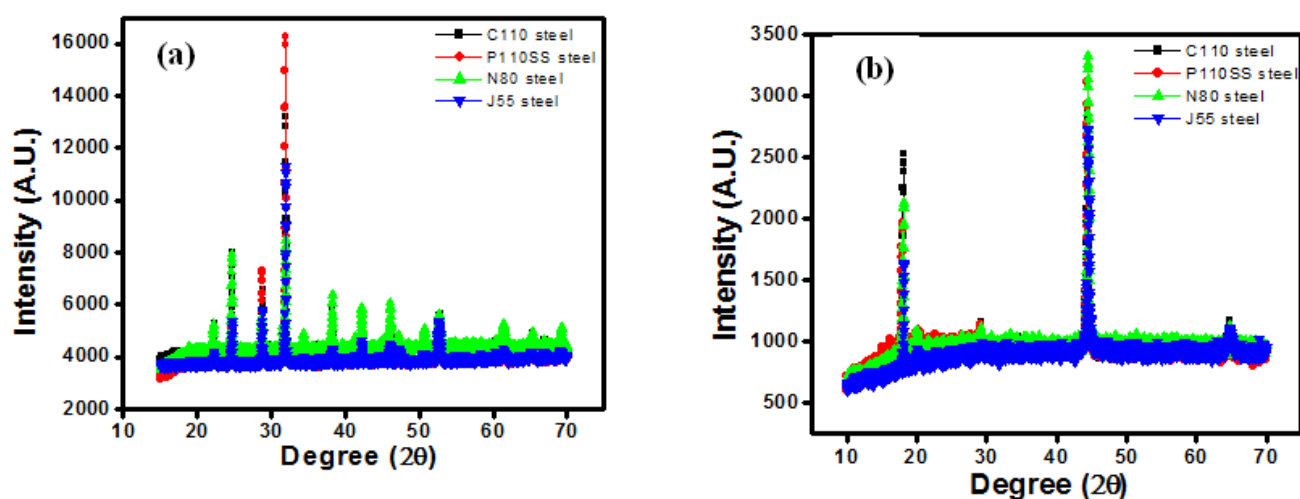


Figure 5. XRD analysis of (a) without berberine extract and (b) after addition of berberine extract.

3.3.3. Contact Angle Measurement

The contact angle measurements were carried out at room temperature. A baseline test without corrosion inhibitor was carried out first after which the corrosion inhibitor package was injected on the carbon steel samples surface and the concentration was increased in steps. Droplets were placed on the steel surface by 10 microliter syringe. For each concentration of corrosion inhibitor the contact angle measurements were repeated 3 times. The contact angle of carbon steel surfaces without inhibitor was measured as $17.4^\circ, 12.6^\circ, 21.4^\circ,$ and 15.5° in the 3.5% NaCl solution; meaning that the wettability of steel surface is hydrophilic (favors water). With the addition of inhibitor the contact angle increased for all carbon steel samples and the steel surface became hydrophobic (does not favors water) as is evident from Figure 6. This confirms the formation of a hydrophobic layer on the steel surface in presence of inhibitor.

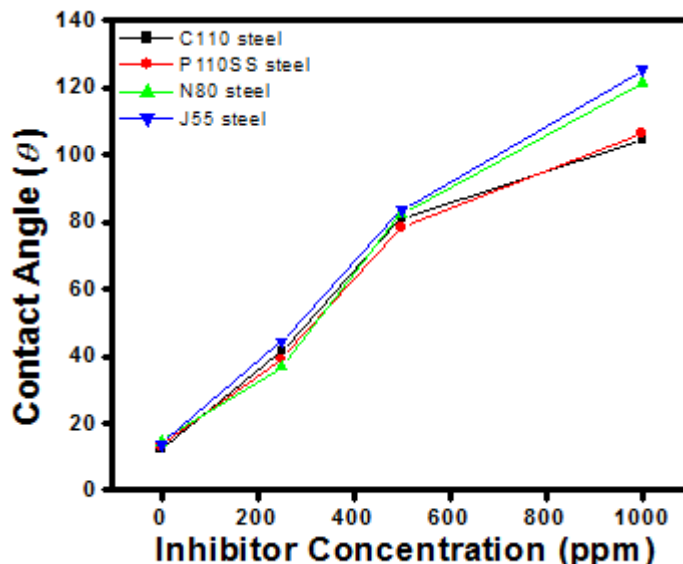
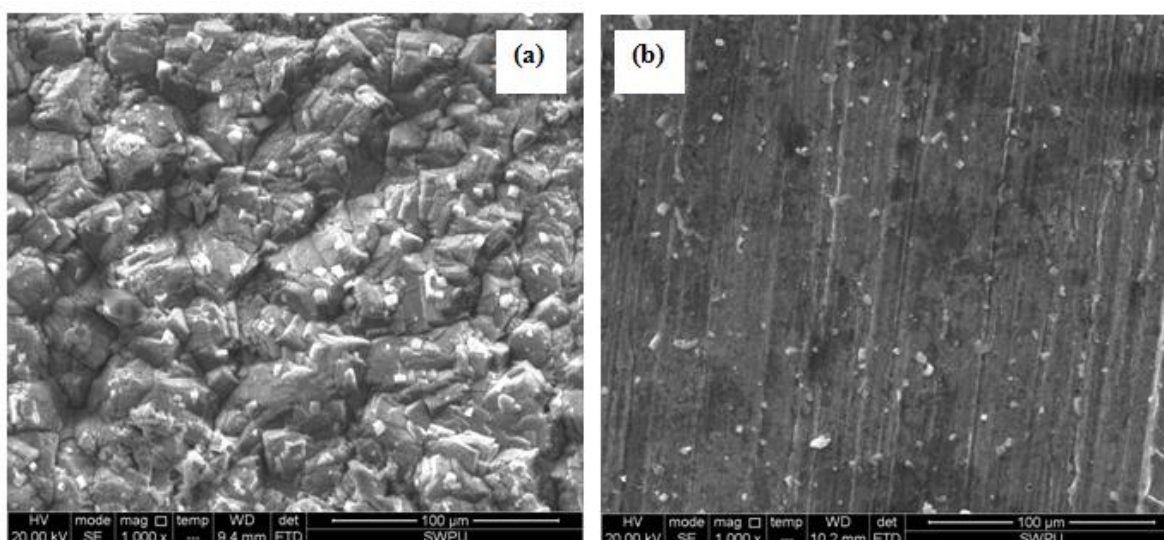


Figure 6. Variation of contact angle with different concentration of berberine extract on carbon steels surface.

3.3.4. Scanning Electron Microscopy (SEM)

Scanning electron microscopy photographs were taken to show the corrosion inhibition is due to the formation of an adsorptive film on the carbon steel surface. The morphology of the C110, N80, P110SS, and J55 steel in Figure 7a, 7c, 7e, and 7g showed a corroded surface in the absence of inhibitors. There are pits and cracks on the specimen’s surface and the surface is strongly damaged. However, in the presence of Berberine extract, the surface corrosion of steel is remarkably decreased. Figure 7b, 7d, 7f, 7h showed a perished surface in 3.5% NaCl solution saturated with CO₂ in presence of Berberine extract. Therefore, a smooth and less corroded morphology of steel samples result from exposure to the inhibitor solutions. These results prove that the Berberine extract formed a protective film on the metal surface and can effectively protect steel samples from a corrosive environment.



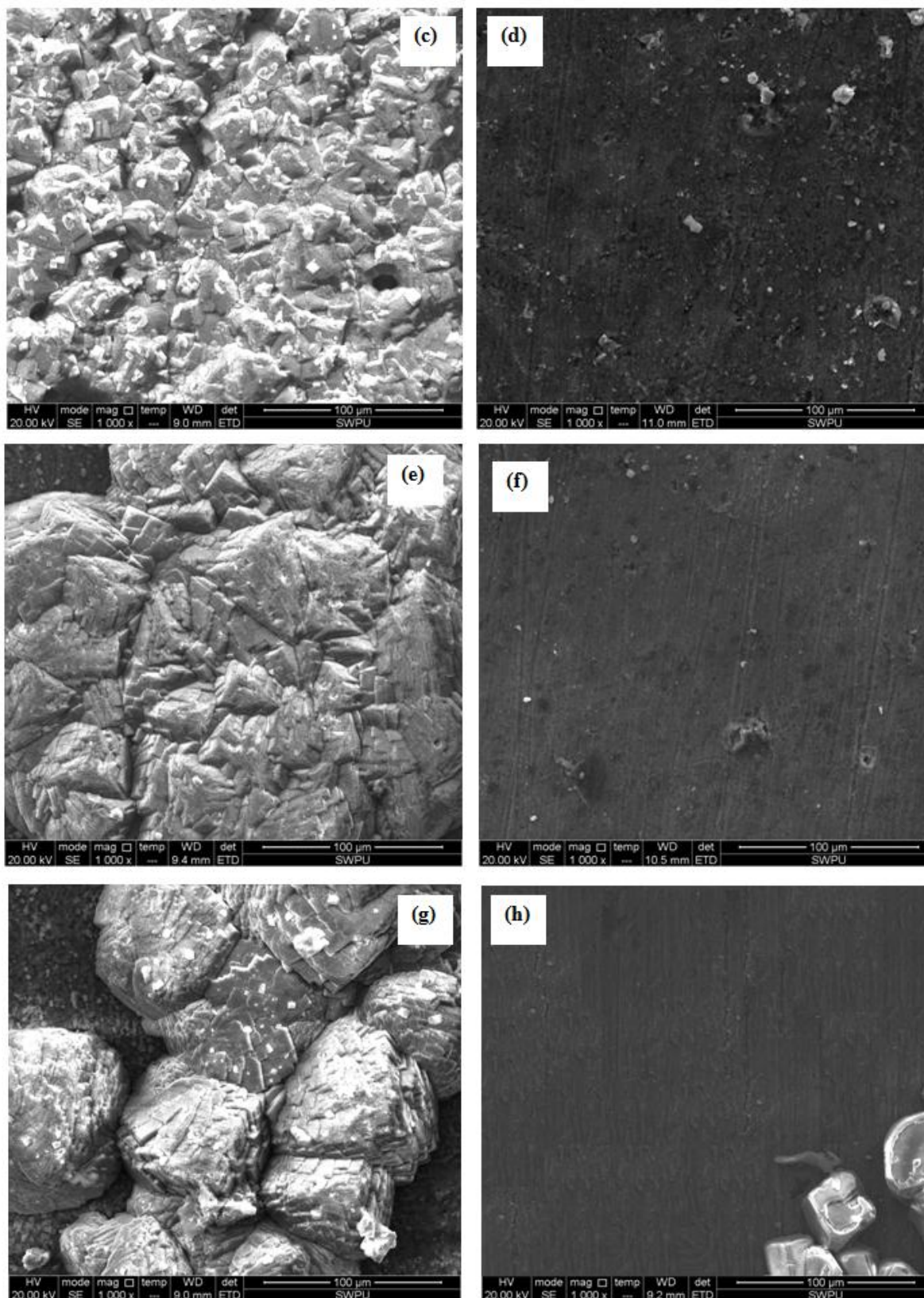
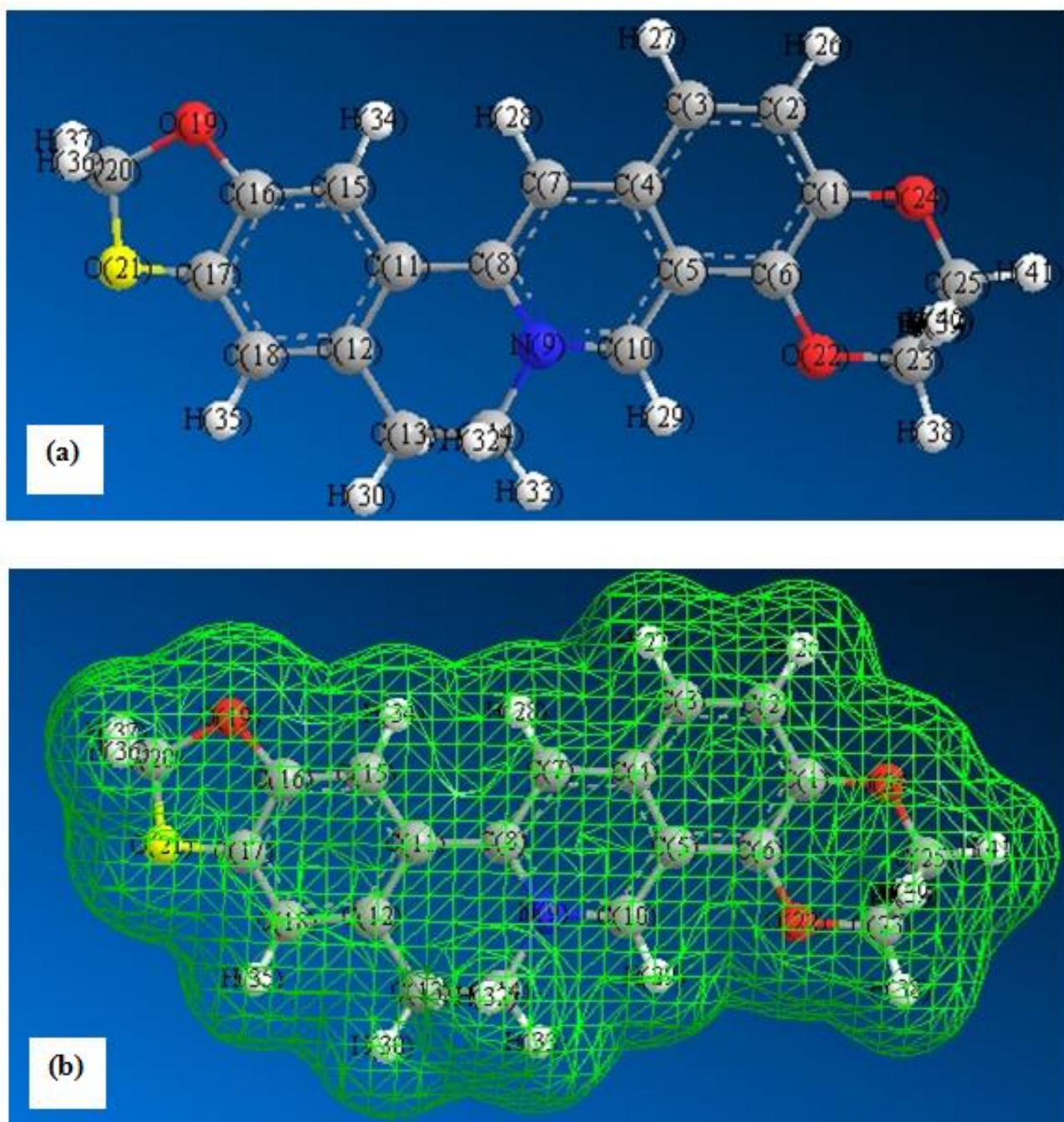


Figure 7. SEM images for (a) 3.5% NaCl solution for C110 steel (b) 1000 ppm berberine extract C110 steel (c) 3.5% NaCl solution for N80 steel (d) 1000 ppm berberine extract N80 steel (e) 3.5% NaCl solution for P110SS steel (f) 1000 ppm berberine extract P110SS steel (g) 3.5% NaCl solution for J55 steel (h) 1000 ppm berberine extract for J55 steel.

3.4. Quantum Chemical Calculations

The structure and electronic parameters were obtained by means of theoretical calculations using the computational methodologies of quantum chemistry. The optimized molecular structures and frontier molecular orbital density distribution of the studied molecule are shown in Figure 8. The calculated quantum chemical parameters such as E_{HOMO} , E_{LUMO} , $\Delta E_{LUMO-HOMO}$, dipole moments (μ) are listed in Table 2. The molecular structure of berberine shows that the molecules seems to adsorb on steel surface by sharing of electrons of the nitrogen and oxygen atoms with iron to form coordinated bonds and π -electron interactions of the aromatic rings.



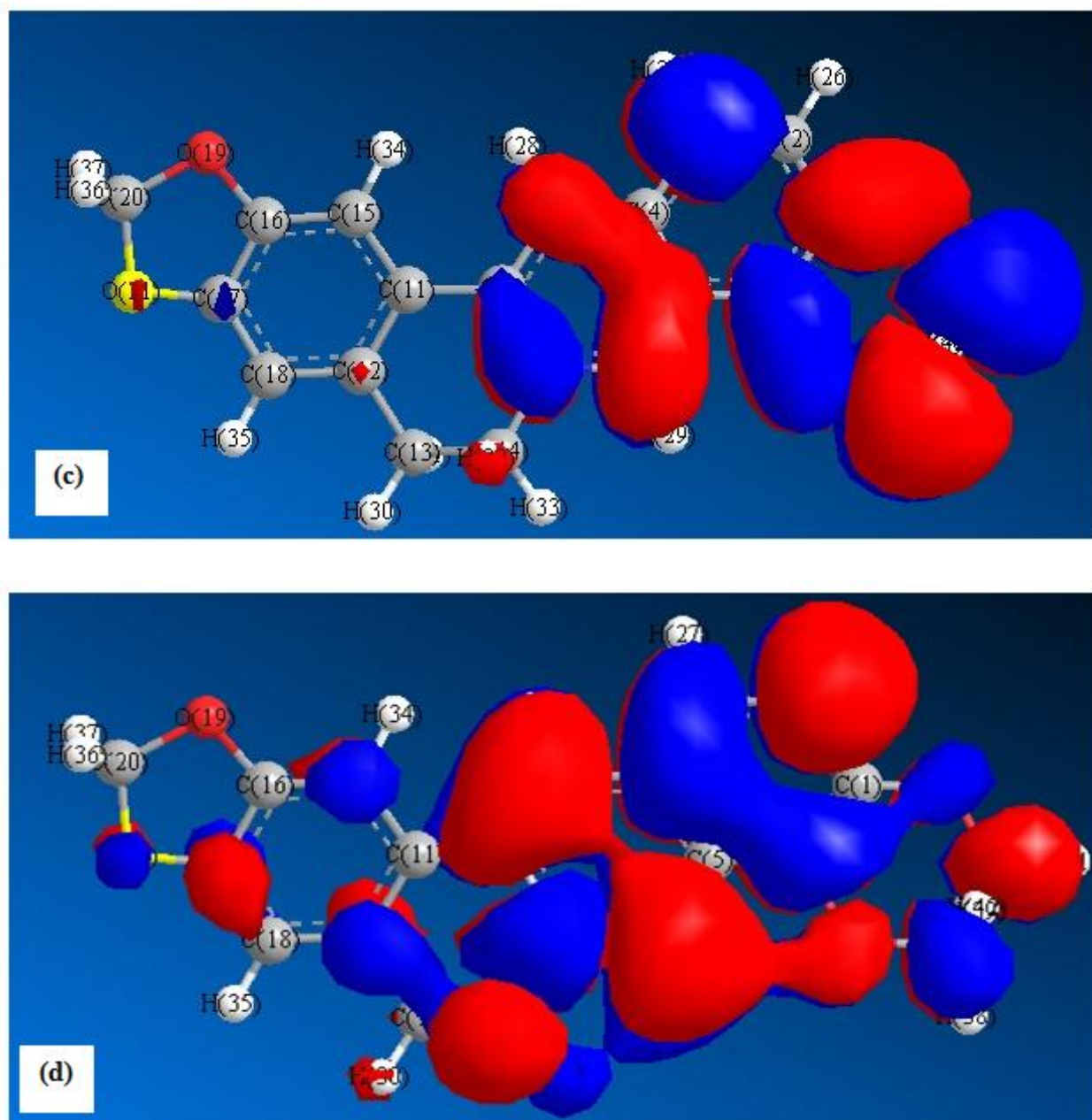


Figure 8. (a) Optimized molecular structure (b) total charge density (c) HOMO (d) LUMO molecular orbital density distribution of Berberine.

Table 2. Calculated quantum chemical parameters of berberine.

Quantum Parameters	Berberine
HOMO (hartree)	-0.27402
LUMO (hartree)	-0.19793
ΔE_{H-L} (hartree)	0.07609
Dipole Moment (μ)	6.5868

The value of highest occupied molecular orbital, E_{HOMO} indicates the tendency of the molecule to donate electrons through nitrogen and oxygen atoms to acceptor molecule with empty and low

energy orbital. E_{LUMO} indicates the tendency of the molecule to accept electrons, with the trend often being that the lower E_{LUMO} is, the greater is the ability of that molecule to accept electrons [15, 16]. The energy gap ΔE is an important parameter that is related to reactivity of the inhibitor molecule towards the metal surface. A high E_{H-L} is associated with a less tendency towards reactivity while a low E_{H-L} is an indication of a great tendency towards reactivity [17- 20]. In this case, berberine showed a strong tendency towards reactivity. Polarity of a covalent bond (Dipole moment μ) can be understood by distribution of electrons in a molecule and large values of dipole moment μ favour the adsorption of inhibitor.

4. MECHANISM OF CORROSION MITIGATION

The inhibition process of steel in the studied environment can be explained by the adsorption of berberine on the metal surface. The adsorption of berberine can be attributed to the presence of N, S and O-atoms and aromatic/heterocyclic rings [21-26]. Therefore, the possible reaction centres are unshared electron pair of hetero-atoms and π - electrons of aromatic/heterocyclic ring. The adsorption and inhibition effect of berberine in 3.5% NaCl solution saturated with CO_2 can be explained as follows: berberine might be protonated in the solution as follows:



Thus, in aqueous solutions, berberine exists either as neutral molecules or in the form of cations (protonated berberine). The neutral berberine may be adsorbed on the metal surface involving the displacement of water molecules from the metal surface. The berberine molecules can be also adsorbed on the metal surface on the basis of donor–acceptor interactions between π -electrons of nitrile group, carbonyl group, and carbon steel samples [27-32]. Also, the berberine molecules may form a hydrophobic film, in contact with the metal surface, thereby retarding corrosion.

5. CONCLUSIONS

1. Berberine extract is a good inhibitor for carbon steels corrosion in 3.5% NaCl solution saturated with CO_2 . Inhibition efficiency increases with increasing inhibitor concentration and inhibition efficiency values obtained from different methods employed are in reasonable agreement.
2. Weight loss results from HPHT autoclave showed that J55 steel exhibited highest inhibition efficiency (96%) while C110 steel exhibited lowest inhibition efficiency (60%) among all the carbon steels.
3. The UV-visible, XRD, contact angle, and SEM analyses showed that the inhibition of carbon steels corrosion occurred due to the formation of a protective film on the metal surface through adsorption of the Berberine molecule.
4. Quantum chemical calculations complemented well the experimental results.

ACKNOWLEDGEMENTS

Authors are thankful for the post doctoral fellowship, financial assistance provided by the National Natural Science Foundation of China (No. 51274170) and the research grants from the Colonel Technology Fund of Southwest Petroleum University (Project No.2012XJZ013).

References

1. W. Bai, J. Yu, Y. Yang, Y. Ye, J. Guo, Y. Zhang, *Int. J. Electrochem. Sci.* 8 (2013) 3441- 3453.
2. J. Han, J. William Carey, J. Zhang, *J. Appl. Electrochem.* 41 (2011) 741-749.
3. B. S. Sanatkumar, J. Nayak, A. N. Shetty, *Int. J. Hydrogen Energ.* 37 (2012) 9431–9442.
4. G. A. Zhang, Y. F. Cheng, *Corros. Sci.* 51, (2009) 87-94.
5. J. Aljourani, K. Raieisi, M. A. Golozar, *Corros. Sci.* 51 (2009) 1836-1843.
6. R. Solmaz, G. Kardaş, M. Çulha, B. Yazici, M. Erbil, *Electrochem. Acta* 53 (2008) 5941-5952.
7. L. Fragoza-Mar, O. Olivares-Xomet, M. A. Domnguez-Aguilar, E. A. Flores, P. Arellanes-Lozada, F. Jiménez-Cruz, *Corros. Sci.* 61 (2012) 171-184.
8. D. K. Yadav, D. S. Chauhan, I. Ahamad, M. A. Quireshi, *RSC Adv.* 3 (2013) 632-646.
9. X. Liu, P. C. Okafor, Y. G. Zheng, *Corros. Sci.* 51 (2009) 744-751.
10. Y. Li, P. Zhao, Q. Liang, B. Hou, *Appl. Surf. Sci.* 252 (2005) 1245-1253.
11. Gaussian 03, Revision E.01, Frisch, M.J.; Trucks, G.W.; Schlegel, H.B.; Scuseria, G.E.; Robb, M.A.; Cheeseman, J.R.; Montgomery, Jr. J.A.; Vreven, T.; Kudin, K.N.; Burant, J.C.; Millam, J.M.; Iyengar, S.S.; Tomasi, J.; Barone, V.; Mennucci, B.; Cossi, M.; Scalmani, G.; Rega, N.; Petersson, G.A.; Nakatsuji, H.; Hada, M.; Ehara, M.; Toyota, K.; Fukuda, R.; Hasegawa, J.; Ishida, M.; Nakajima, T.; Honda, Y.; Kitao, O.; Nakai, H.; Klene, M.; Li, X.; Knox, J.E.; Hratchian, H.P.; Cross, J.B.; Bakken, V.; Adamo, C.; Jaramillo, J.; Gomperts, R.; Stratman, R.E.; Yazyev, O.; Austin, A.J.; Cammi, R.; Pomelli, C.; Ochterski, J.W.; Ayala, P.Y.; Morokuma, K.; Voth, G.A.; Salvador, P.; Dannenberg, J.J.; Zakrzewski, V.G.; Dapprich, S.; Daniels, A.D.; Strain, M.C.; Farkas, O.; Malick, D.K.; Rabuck, A.D.; Raghavachari, K.; Foresman, J.B.; Ortiz, J.V.; Cui, Q.; Baboul, A.G.; Clifford, S.; Cioslowski, J.; Stefanov, B.B.; Liu, G.; Liashenko, Piskorz, A. P.; Komaromi, I.; Martin, R.L.; Fox, D.J.; Keith, T.; Al-Laham, M.A.; Peng, C.Y.; Nanayakkara, A.; Challacombe, M.; Gill, P.M.W.; Johnson, B.; Chen, W.; Wong, M.W.; Gonzalez, C.; Pople, J.A.; Gaussian, Inc., Wallingford CT, 2003.
12. G. Ji, S. K. Shukla, P. Dwivedi, S. Sundaram, R. Prakash, *Ind. Eng. Chem. Res.* 50 (2011) 11954-11959.
13. Y. Abboud, B. Hammouti, A. Abourriche B. Ihssane, A. Bennamar, M. Charroufi, S. S. Al-Deyab, *Int. J. Electrochem. Sci.* 7 (2012) 2543-2551.
14. Y. Abboud, B. Hammouti, A. Abourriche, A. Bennamara, H. Hannache, *Res. Chem. Intermed.* 38 (2012) 1591-1607.
15. D. K. Yadav, M. A. Quraishi, *Ind. Eng. Chem. Res.* 51 (2012) 14966-14979.
16. D. K. Yadav, M. A. Quraishi, B. Maiti, *Corros. Sci.* 55 (2011) 254-266.
17. A. Singh, M. A. Quraishi, E. E. Ebenso, *Int. J. Electrochem. Sci.* 7 (2012) 12545 - 12557.
18. M. M. Kabanda, I. B. Obot, Eno E. Ebenso, *Int. J. Electrochem. Sci.* 8 (2013) 10839-10850.
19. Gökhan Gece, S. Bilgic, *Corros. Sci.* 51 (2009) 1876-1878.
20. P. B. Raja, A. K. Qureshi, A. A. Rahim, H. Osman, K. Awang, *Corros. Sci.* 69 (2013) 292-301.
21. M. A. Quraishi, A. Singh, V. K. Singh, D. K. Yadav, A. K. Singh, *Mater. Chem. Phys.* 122 (2010) 114-122.
22. A. Singh, I. Ahamad, V. K. Singh, M. A. Quraishi, *J. Solid State Electrochem.* 15 (2011) 1087-1097.
23. Ismail, K. M. *Electrochem. Acta.* 2008, 53, 5953-5960.
24. M. A. Chidiebere, C. E. Ogukwe, K. L. Oguzie, C N. Eneh, E. E. Oguzie, *Ind. Eng. Chem. Res.* 51 (2012) 668-677.

25. I. Ahamad, R. Prasad, M. A. Quraishi, *J. Solid State Electrochem.* 14 (2010) 2095-2105.
26. A. Lecante, F. Robert, P. A. Blandini_eres, C. Roos, *Curr. Appl. Phys.* 11 (2011) 714-724.
27. A. Singh, I. Ahamad, M. A. Quraishi, *Arab. J. Chem.* (2013) <http://dx.doi.org/10.1016/j.arabjc.2012.04.029>.
28. S. A. Umoren, I. B. Obot, E. E. Ebenso, N. O. Obi-Egbedi, *Desal.* 247 (2009) 561-572.
29. A. Yurt, O. Aykın, *Corros. Sci.* 53 (2011) 3725-3732.
30. A. Khamis, M.M. Saleh, M.I. Awad, *Corros. Sci.* 66 (2013) 343-349.
31. M. Lashgari, A. M. Malek, *Electrochem. Acta* 55 (2010) 5253-5257.
32. H. Gerengi, *Ind. Eng. Chem. Res.* 51 (2012) 12835-12843.

© 2015 The Authors. Published by ESG (www.electrochemsci.org). This article is an open access article distributed under the terms and conditions of the Creative Commons Attribution license (<http://creativecommons.org/licenses/by/4.0/>).